Regular Article

MYELOID NEOPLASIA

Mutant IDH1 promotes leukemogenesis in vivo and can be specifically targeted in human AML

Anuhar Chaturvedi,[1] Michelle Maria Araujo Cruz,[1] Nidhi Jyotsana,[1] Amit Sharma,[1] Haiyang Yun,[1] Kerstin Görlich,[1] Martin Wichmann,[1] Adrian Schwarzer,[2] Matthias Preller,[3] Felicitas Thol,[1] Johann Meyer,[2] Reinhard Haemmerle,[2] Eduard A. Struys,[4] Erwin E. Jansen,[4] Ute Modlich,[2] Zhixiong Li,[2] Laura M. Sly,[5] Robert Geffers,[6] Robert Lindner,[7] Dietmar J. Manstein,[3] Ulrich Lehmann,[8] Jürgen Krauter,[1] Arnold Ganser,[1] and Michael Heuser[1]

[1]Department of Hematology, Hemostasis, Oncology, and Stem Cell Transplantation, [2]Institute of Experimental Hematology, and [3]Institute for Biophysical Chemistry and Research Division for Structural Analysis, Hannover Medical School, Hannover, Germany; [4]Department of Clinical Chemistry, Vrije Universiteit University Medical Center, Amsterdam, The Netherlands; [5]Child and Family Research Institute, University of British Columbia, Vancouver, BC, Canada; [6]Department of Cell Biology and Immunology, Helmholtz Centre for Infection Research, Braunschweig, Germany; and [7]Institute of Cell Biology, and [8]Institute of Pathology, Hannover Medical School, Hannover, Germany

Key Points

- IDH1 promotes leukemogenesis in vivo in cooperation with HoxA9.
- Pharmacologic inhibition of mutant IDH1 efficiently inhibits AML cells of IDH1-mutated patients but not of normal CD34$^+$ bone marrow cells.

Mutations in the metabolic enzymes isocitrate dehydrogenase 1 (IDH1) and 2 (IDH2) are frequently found in glioma, acute myeloid leukemia (AML), melanoma, thyroid cancer, and chondrosarcoma patients. Mutant IDH produces 2-hydroxyglutarate (2HG), which induces histone- and DNA-hypermethylation through inhibition of epigenetic regulators. We investigated the role of mutant IDH1 using the mouse transplantation assay. Mutant IDH1 alone did not transform hematopoietic cells during 5 months of observation. However, mutant IDH1 greatly accelerated onset of myeloproliferative disease–like myeloid leukemia in mice in cooperation with HoxA9 with a mean latency of 83 days compared with cells expressing HoxA9 and wild-type IDH1 or a control vector (167 and 210 days, respectively, $P = .001$). Mutant IDH1 accelerated cell-cycle transition through repression of cyclin-dependent kinase inhibitors Cdkn2a and Cdkn2b, and activated mitogen-activated protein kinase signaling. By computational screening, we identified an inhibitor of mutant IDH1, which inhibited mutant IDH1 cells and lowered 2HG levels in vitro, and efficiently blocked colony formation of AML cells from IDH1-mutated patients but not of normal CD34$^+$ bone marrow cells. These data demonstrate that mutant IDH1 has oncogenic activity in vivo and suggest that it is a promising therapeutic target in human AML cells. (Blood. 2013;122(16):2877-2887)

Introduction

Mutations in isocitrate dehydrogenase 1 (IDH1) and IDH2 were originally identified in glioma,[1,2] acute myeloid leukemia (AML), myeloproliferative neoplasm, and myelodysplastic (MDS) syndrome patients[3-5] but are increasingly found in a diverse set of other tumor entities such as chondrosarcoma,[6] lymphoma,[7] melanoma,[8] and thyroid cancer.[9] In cytogenetically normal AML, mutated IDH1 is found in 10.9% of patients,[10] whereas mutated IDH2 is found in 12.1%.[11] Mutations in IDH1 are almost exclusively found at amino acid arginine 132,[12] and IDH2 mutations are found more frequently at position R140 and less frequently at position R172.[13] All mutations affect the active site of the enzymes where isocitrate and reduced NAD phosphate bind.[14-16] Whereas the enzymatic function of mutant IDH to convert isocitrate to α-ketoglutarate is impaired, it gains a neomorphic function to convert α-ketoglutarate to R-2-hydroxyglutarate (R-2HG, also known as D-2HG).[14-16]

Genome-wide methylation studies revealed a strong association of mutant IDH1 with an increased number of methylated cytosine guanine dinucleotide (CpGs).[17] Similarly, AML patients with mutant TET2 showed a higher number of methylated CpGs, whereas IDH and TET2 mutations almost never occur in the same patient.[17] This observation led to the hypothesis that mutant IDH inhibits TET2 function, thus leading to increased DNA methylation and leukemia.[17] Indeed, the metabolite 2HG was shown to inhibit the function of TET2, resulting in DNA hypermethylation.[18] Many other α-ketoglutarate–dependent dioxygenases and histone demethylases are competitively blocked by 2HG.[17-21] Interestingly, a recent study showed that R-2HG, but not S-2-hydroxyglutarate (S-2HG), promotes cytokine independence of a leukemia cell line through activation of the EglN1 prolyl hydroxylase.[19,22]

There is an Inside Blood commentary on this article in this issue.

Several studies suggested that mutant IDH1 and specifically 2HG block myeloid and adipocyte differentiation.[17,20] The biological function of mutant IDH1 has been recently studied in a knock-in mouse model, demonstrating an increase in the number of hematopoietic progenitor cells and increased cell proliferation and splenomegaly.[23] Mutant mice did not develop leukemia and had a similar survival as wild-type mice, suggesting that mutant IDH1 alone is not sufficient to induce leukemia.[23] Potentially collaborating genes in AML patients are mutant *NPM1* and *FLT3*; these mutations frequently co-occur with mutant *IDH*.[24] Xu et al demonstrated that expression of *HoxA* genes was increased in *IDH1* mutated cells.[18]

To identify potentially collaborating partners of mutant IDH1, we investigated the ability of other oncogenes to collaborate with mutant IDH1 in leukemogenesis.

Materials and methods

More information on materials and methods can be found in the supplemental information on the *Blood* website.

Retroviral vectors and vector production

Retroviral vectors MSCV-PGKneo,[25] MSCV-*HoxA9*-PGKneo,[25] and pSF91-IRES-eGFP[26] have been described previously. pSF91-IRES-eGFP has been modified for Gateway cloning by inserting the RfA cassette (Invitrogen-Life Technologies, Darmstadt, Germany) as described.[27] The 1.2-kb coding region of human *IDH1* was amplified by nested polymerase chain reaction (PCR) from complementary DNA of bone marrow cells from an MDS syndrome patient with a heterozygous *IDH1*R132C mutation. Helper-free recombinant retrovirus produced in supernatants of transfected ecotropic Phoenix packaging cell line was used to transduce the ecotropic GP+E86 packaging cell line.[28]

Mice and retroviral infection of primary bone marrow cells

Six- to 8-week-old female C57BL/6J mice were purchased from Charles River, Sulzfeld, Germany, and kept in pathogen-free conditions at the central animal laboratory of Hannover Medical School. All animal experiments were approved by the Lower Saxony state office for consumer protection, Oldenburg, Germany. Primary mouse bone marrow cells were transduced as previously described.[29]

Bone marrow transplantation and monitoring of mice

Equal numbers of green fluorescent protein (GFP)-expressing, sorted bone marrow cells from C57BL/6J mice were injected intravenously in lethally irradiated syngeneic recipient mice that were irradiated with 800 cGy, accompanied by a life-sparing dose of 1×10^5 freshly isolated bone marrow cells from syngeneic mice. Donor chimerism was monitored by tail vein bleeds and fluorescence-activated cell sorter (FACS) analysis of GFP-expressing cells every 4 weeks as previously described.[30] Blood counts with differential white blood cell analysis were performed using an ABC Vet Automated Blood counter (Scil animal care company GmbH, Viernheim, Germany). Lineage distribution was determined by FACS analysis (FACS Calibur; Becton Dickinson, Heidelberg, Germany) as previously described.[29]

Clonogenic progenitor assay

Colony-forming cell (CFC) units were assayed in methylcellulose (Methocult M3234; StemCell Technologies, Inc., Vancouver, BC, Canada) as described in supplemental Methods.

Patient samples and CD34+ cells

Diagnostic bone marrow or peripheral blood samples were analyzed from 400 adult patients (16-60 years) with de novo or secondary AML (FAB M0-M2, M4-M7) who had entered the multicenter treatment trial AML-SHG 01/99 or 02/95 for mutations in *IDH1* as previously described.[10] The association of *IDH1* mutations with expression levels of *HOXA* and *HOXB* cluster genes in adult AML patients up to 60 years of age were studied in 457 patients of the Hemato-Oncology Cooperative study group.[31] The association of *IDH1* mutations with *HOXA9* was studied in an independent cohort.[32] In brief, HG-U133-plus2 microarray data of 197 AML patients were downloaded from The Cancer Genome Atlas Data Portal (https://tcga-data.nci.nih.gov/tcga/).[32] The normalized intensity signals of the 2 *HOXA9*-specific probes were extracted and $\log_2$ transformed. Bone marrow of healthy donors was obtained from the transplantation unit of Hannover Medical School. CD34+ cells were isolated using the CD34 microbead kit (Miltenyi Biotech, Bergisch Gladbach, Germany) per the manufacturer's protocol. Written informed consent was obtained according to the Declaration of Helsinki, and the study was approved by the institutional review board of Hannover Medical School.

2-hydroxyglutarate measurement

To determine intracellular *R*- and S-2HG levels, 5-10 million cells were sonicated for 10 minutes at intervals of 30 seconds on, 30 seconds off at 4°C using the Bioruptor (Diagenode, Liege, Belgium) followed by 2 rounds of freeze–thaw cycles. All analyses were performed on an AB Sciex 4000 Q-trap triple quadruple mass spectrometer (Applied Biosystems, Darmstadt, Germany). Liquid chromatography was performed on an Xterra C_{18} analytical column (150 × 3.9 mm [inner diameter]; 5-μm bead size) with water–acetonitrile (96.5:3.5 by volume) containing 125 mg/L ammonium formate (pH adjusted to 3.6 by addition of formic acid) as mobile phase as described.[33]

Cell-cycle analysis in vitro and in vivo

For cell-cycle analysis, mice were injected intraperitoneally (IP) with 100 μL 5-bromo-2′-deoxyuridine (BrdU) (1 mM) at 36, 24, and 12 hours before harvest. For in vitro labeling, 10 μM of BrdU was added to 1 million cells for 6 hours. Cell-cycle analysis was performed according to the manufacturer's protocol (BD Pharmingen, catalog no. 557892).

Apoptosis measurement

Cells were stained with Annexin V-APC and 7AAD according to the manufacturer's protocol (BD Pharmingen; catalog no. 550474).

Immunoblotting

Cellular lysates were prepared and immunoblotting was performed as described previously.[34] Antibodies and methods are described in the supplemental Methods.

Quantitative RT-PCR

RNA was extracted and reverse transcribed as previously described.[35] Quantitative reverse-transcriptase (RT)-PCR was done as previously described using SYBR green (Invitrogen) for quantification of double-stranded DNA on a StepOne Plus cycler (Applied Biosystems).[36] Relative expression was determined with the $2^{-\Delta\Delta CT}$ method,[37] and the housekeeping gene transcript *Abl1* was used to normalize the results.

Methylation analysis

Genomic DNA was isolated from cells using the Allprep DNA RNA kit (Qiagen, Hilden, Germany). One μg of genomic DNA was bisulfite converted with the EZ DNA Methylation kit (Zymo Research, Freiburg, Germany). A PCR amplification of 50-100 ng equivalent of the starting amount of converted DNA was performed with C to T conversion-specific primers, cloned in pCR2.1-TOPO sequencing vector (Invitrogen), and sequenced by Sanger sequencing.
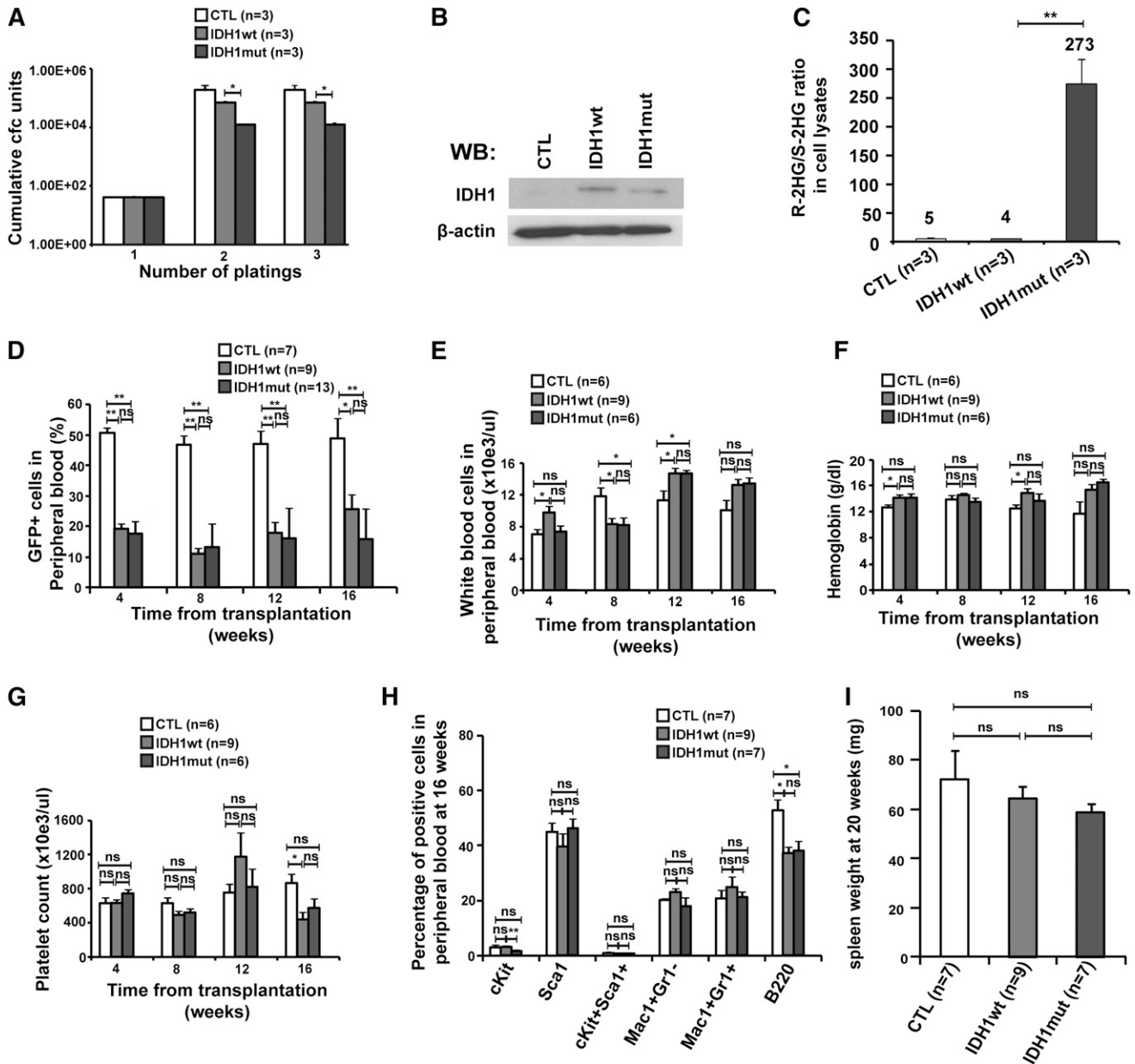
Figure 1. Effect of constitutive expression of mutated IDH1 in primary bone marrow cells in vitro and in vivo. (A) Cumulative CFC yield is shown for an initial plating of 1000 transgene-expressing cells (cells were sorted before plating; mean ± SEM of 3 independent experiments). (B) Protein expression of mouse bone marrow cells transduced with a CTL vector or with FLAG-tagged wild-type IDH1 or mutant IDH1 using an anti-FLAG antibody. Cells were harvested from bone marrow 4 weeks after transplantation. β-actin was probed on the same blot as a loading control. (C) Ratio of R-2HG to S-2HG in mouse bone marrow cells transduced with CTL vector or with wild-type or mutant IDH1. Cells were harvested from bone marrow 4 weeks after transplantation (mean ± standard error of the mean [SEM] of 3 independent mice). (D) Engraftment of transduced cells in peripheral blood at different time points after transplantation of 1×10^5 transgene-positive cells (mean ± SEM). (E) White blood cell count in peripheral blood at different time points after transplantation of control or IDH1-transduced bone marrow cells (mean ± SEM). (F) Hemoglobin levels in peripheral blood at different time points after transplantation of control or IDH1-transduced bone marrow cells (mean ± SEM). (G) Platelet count in peripheral blood at different time points after transplantation of control or IDH1-transduced bone marrow cells (mean ± SEM). (H) Immunophenotype of transduced cells in peripheral blood at 16 weeks after transplantation (mean ± SEM). (I) Average spleen weight in mice receiving transplants of control or IDH1-transduced bone marrow cells 20 weeks after transplantation (mean ± SEM). *P < .05; **P < .01; ns, not significant. WB, western blot.

Gene expression profiling

GFP$^+$ cells were sorted from mouse bone marrow cells 4 weeks after transplantation and were hybridized to an identical lot of Affymetrix GeneChips. Further details are described in the supplemental Methods. Gene expression profiling data can be found at the Gene Expression Omnibus database (accession number GSE45019).

In vitro cytotoxicity assay

Cells were plated at a density of 5×10^4 cells/mL in flat bottom 96-well plates (100 μL/well) and incubated under light protective conditions. The drugs were

added to the culture medium at the specified concentrations. After 64 hours, 10 μL alamarBlue (Abd Serotec, Raleigh, NC) was added per well. Fluorescence intensity was measured after 72 hours on a microplate reader (Safire; Tecan, Männedorf, Switzerland). All experiments were performed in duplicate with 3 independently transduced cell lines.

H$_2$O$_2$ measurement

The measurement of hydrogen peroxide was carried out using the Amplex-red hydrogen peroxide/peroxidase assay kit as described by the manufacturer (Molecular Probes, Invitrogen, Darmstadt, Germany).
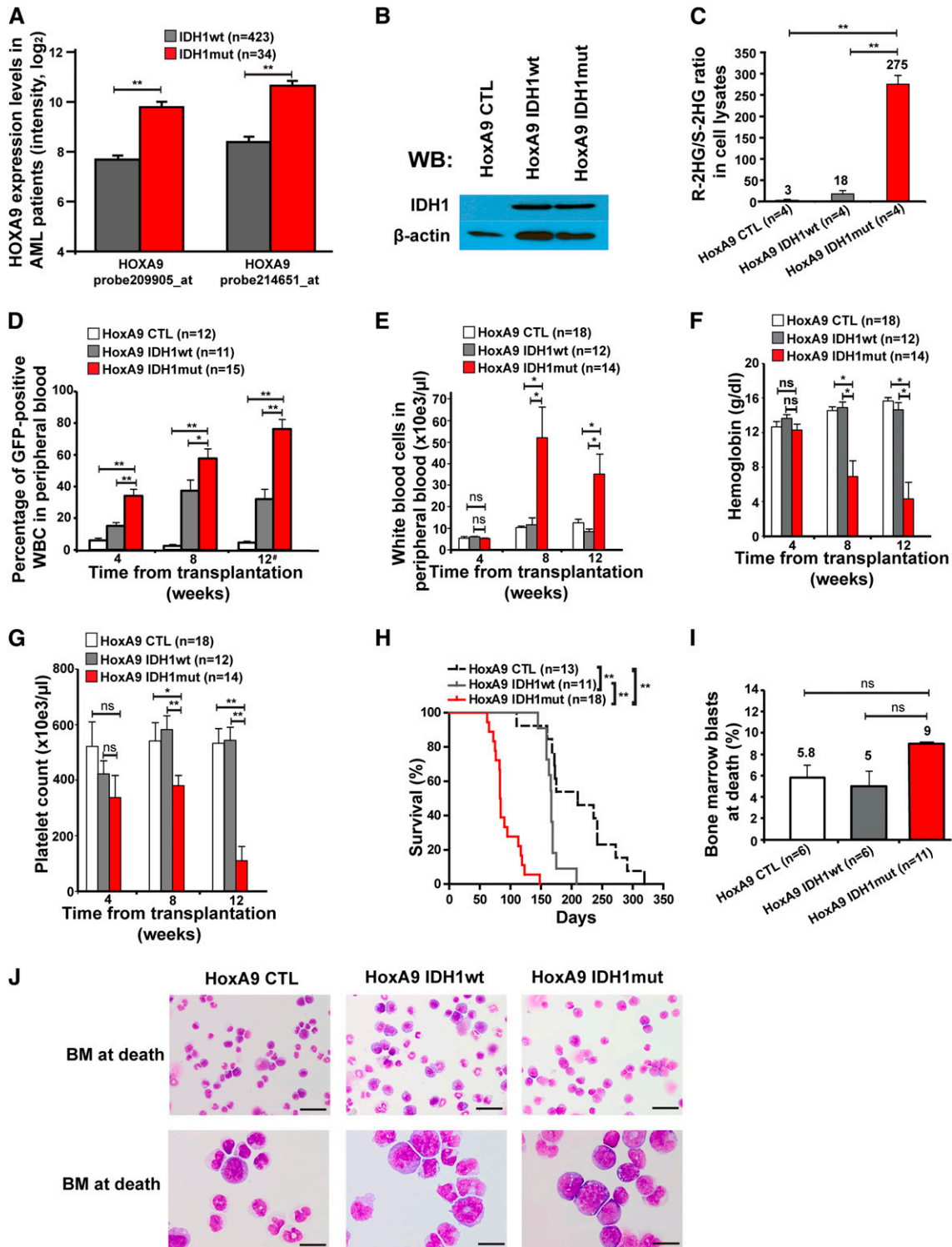
Figure 2. Mutant IDH1 induces a myeloproliferative-like disease in immortalized bone marrow cells. (A) Association of *IDH1* mutations with expression levels of *HOXA9* in adult AML patients up to 60 years of age (n = 457). Normalized expression levels of *HOXA9* are shown for patients with wild-type IDH1 (gray bars) and mutant IDH1 (red bars), which were determined on an Affymetrix microarray with 2 different probes.[31] (B) Protein expression of HoxA9-immortalized cells transduced with a CTL vector or with FLAG-tagged wild-type IDH1 or mutant IDH1 using an anti-FLAG antibody. β-actin was probed on the same blot as a loading control. (C) Ratio of *R*-2HG to S-2HG in cultured HoxA9 cells transduced with CTL, IDH1wt, or IDH1mut (mean ± SEM of 4 independently transduced cell lines). (D) Engraftment of transduced cells in peripheral blood at different time points after transplantation of 1×10^6 transgene-positive cells (mean ± SEM of the indicated number of mice). #For mice that died before week 12, engraftment in peripheral blood is shown for the time point of death. (E) White blood cell count in peripheral blood from mice that received transplants of cells transduced with the indicated constructs. Blood was taken 4, 8, and 12 weeks after transplantation (mean ± SEM of the indicated number of mice). (F) Hemoglobin level in peripheral blood from mice that received transplants of cells transduced with the indicated constructs. Blood was taken 4, 8, and 12 weeks after transplantation (mean ± SEM of the indicated number of mice). (G) Platelet counts in peripheral blood from mice that received transplants of cells transduced with the indicated constructs. Blood was taken 4, 8, and 12 weeks after transplantation (mean ± SEM of the indicated number of mice). (H) Survival of mice that received transplants of cells transduced with the indicated constructs. Results from 3 independent experiments using independently transduced cells are shown. (I) Percentage of blast cells in bone marrow of moribund mice (mean ± SEM of the indicated number of mice). (J) Representative Wright-Giemsa–stained cytospin preparations of bone marrow cells from moribund mice (Scale bar: 25 μm in the upper panel; Scale bar: 10 μm in the lower panel). *P < .05; **P < .01; ns, not significant.
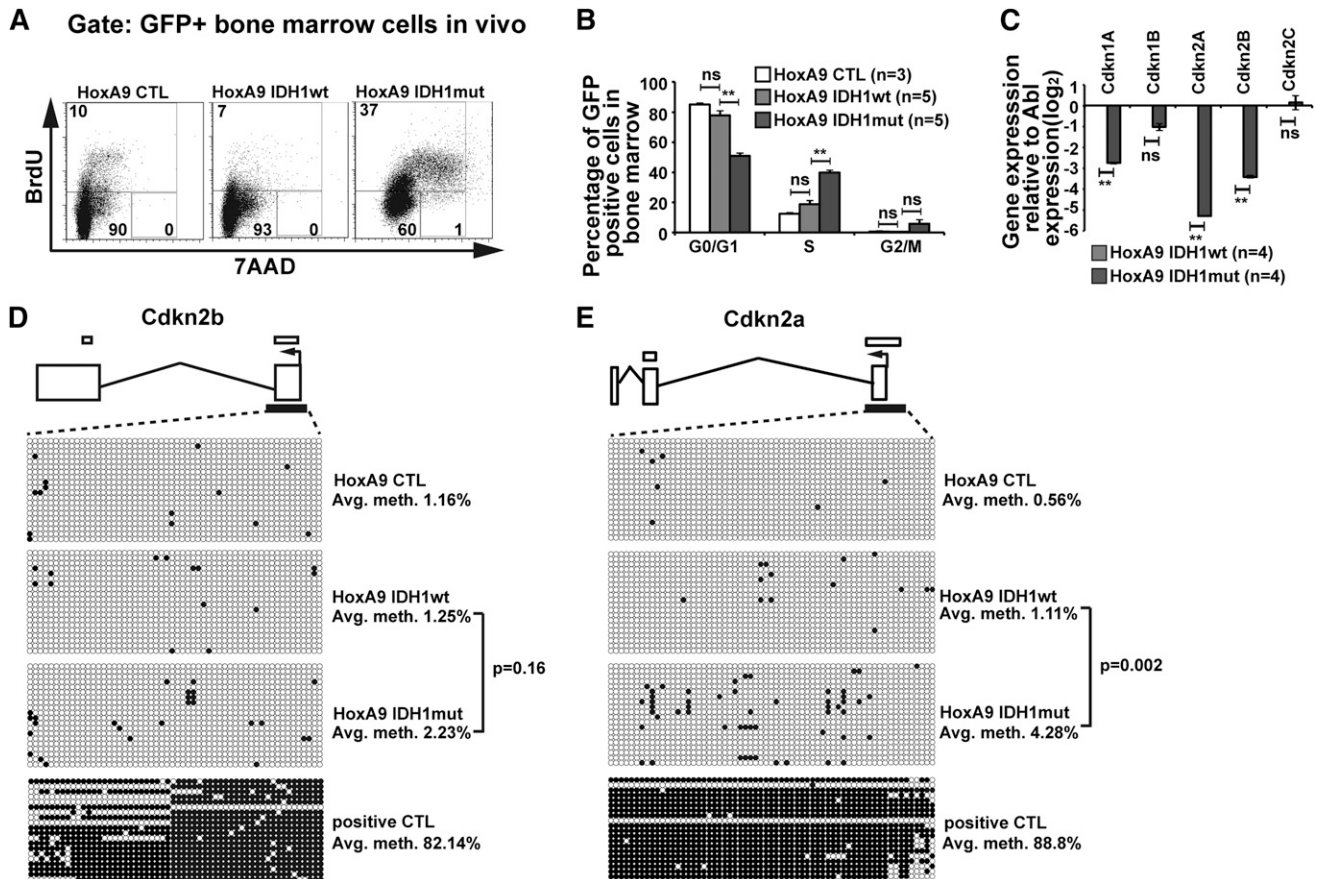
Figure 3. Mutant IDH1 promotes cell-cycle transition independently of 2-hydroxyglutarate. (A) Representative FACS blots of cell-cycle phases in HoxA9-immortalized vector CTL, IDH1wt, or IDH1mut transduced (GFP$^+$) bone marrow cells 9 weeks after transplantation (BrdU injections IP at 36, 24, and 12 hours before harvest). Cell-cycle phases were determined by analysis of BrdU/7AAD-stained cells by FACS. The upper quadrant represents cells in S phase; the lower left quadrant represents cells in G0/G1 phase; and the lower right quadrant represents cells in G2/M phase of the cell cycle. (B) Cell-cycle distribution in HoxA9-immortalized vector CTL, IDH1wt, and IDH1mut transduced (GFP$^+$) bone marrow cells 9 weeks after transplantation (BrdU injections IP at 36, 24, and 12 hours before harvest). Cell-cycle phases were determined by analysis of BrdU/7AAD-stained cells by FACS (mean ± SEM). (C) Gene expression levels of cyclin-dependent kinase inhibitors in in vitro–cultured HoxA9 cells transduced with IDH1wt and IDH1mut. Gene expression was determined by RT-PCR relative to the housekeeping gene Abl and was normalized to gene expression in IDH1wt cells (mean ± SEM). (D) Methylation analysis of the CpG island in the *Cdkn2b* (p15) promoter in Hoxa9 cells transduced with *IDH1*wt and *IDH1*mut. DNA from in vitro–cultured cells was extracted and bisulfite treated. CpG methyltransferase-treated DNA from IDH1mut cells served as a positive control. The p15 promoter CpG was amplified and subcloned. Twenty clones were sequenced per cell type. Exons are represented by vertical rectangles. White horizontal bars above the exons show CpG islands; black horizontal bars below the exons show the tested region. An open circle indicates a nonmethylated CpG; a black circle indicates a methylated CpG. The percent methylation of the CpG island is calculated by the proportion of methylated CpGs from all investigated CpGs. (E) Methylation analysis of the CpG island in the *Cdkn2a* (p16) promoter in *Hoxa9* cells transduced with IDH1wt and IDH1mut. The analysis was performed as described in the Figure 3D legend. *$P < .05$; **$P < .01$; ns, not significant.

Computational screening

IDH1mut crystal structure in the closed conformation (Protein Data Bank ID code 3INM) was built using Modeler.[38] HMS-101 was identified by in silico drug screening of approximately 500 000 compounds against mutant IDH1 using compounds of the ZINC database.[39]

Statistical analysis

Pairwise comparisons were performed by Student *t* test for continuous variables and by χ-squared test for categorical variables. The 2-sided level of significance was set at $P < .05$. Comparison of survival curves were performed using the log-rank test. A binary logistic regression model was used to analyze associations between mutation status of *IDH1*, *NPM1*, *FLT3*, *CEBPA*, and expression levels *HOXA9*. Statistical analyses were performed with Microsoft Excel (Microsoft, Munich, Germany), GraphPad Prism 5 (GraphPad Software, La Jolla, CA), or SPSS 20.0 (IBM Deutschland, Ehningen, Germany). Graphical representation was prepared using Adobe Illustrator CS5.1 (Adobe Systems GmbH, Munich, Germany).

Results

Mutant IDH1 induces a myeloproliferative-like disease in immortalized bone marrow cells

To test whether mutant IDH1 induces a myeloid malignancy, we cloned *IDH1*wt and *IDH1*mut from a patient with MDS syndrome and transduced control (CTL), *IDH1*wt, or *IDH1*mut constructs in 5-fluorouracil pretreated bone marrow cells. The cumulative CFC yield from sorted transgene positive cells was not increased and the cells stopped proliferating after the second replating (Figure 1A).

We transduced 5-fluorouracil pretreated bone marrow cells with CTL, wild-type, and mutant *IDH1* constructs and confirmed transgene expression in bone marrow cells 4 weeks after transplantation (Figure 1B). A high ratio of *R*-2HG to *S*-2HG was observed in bone marrow cell lysates from IDH1mut transduced cells compared with IDH1wt , or control cells (Figure 1C). In vivo, when transplanting
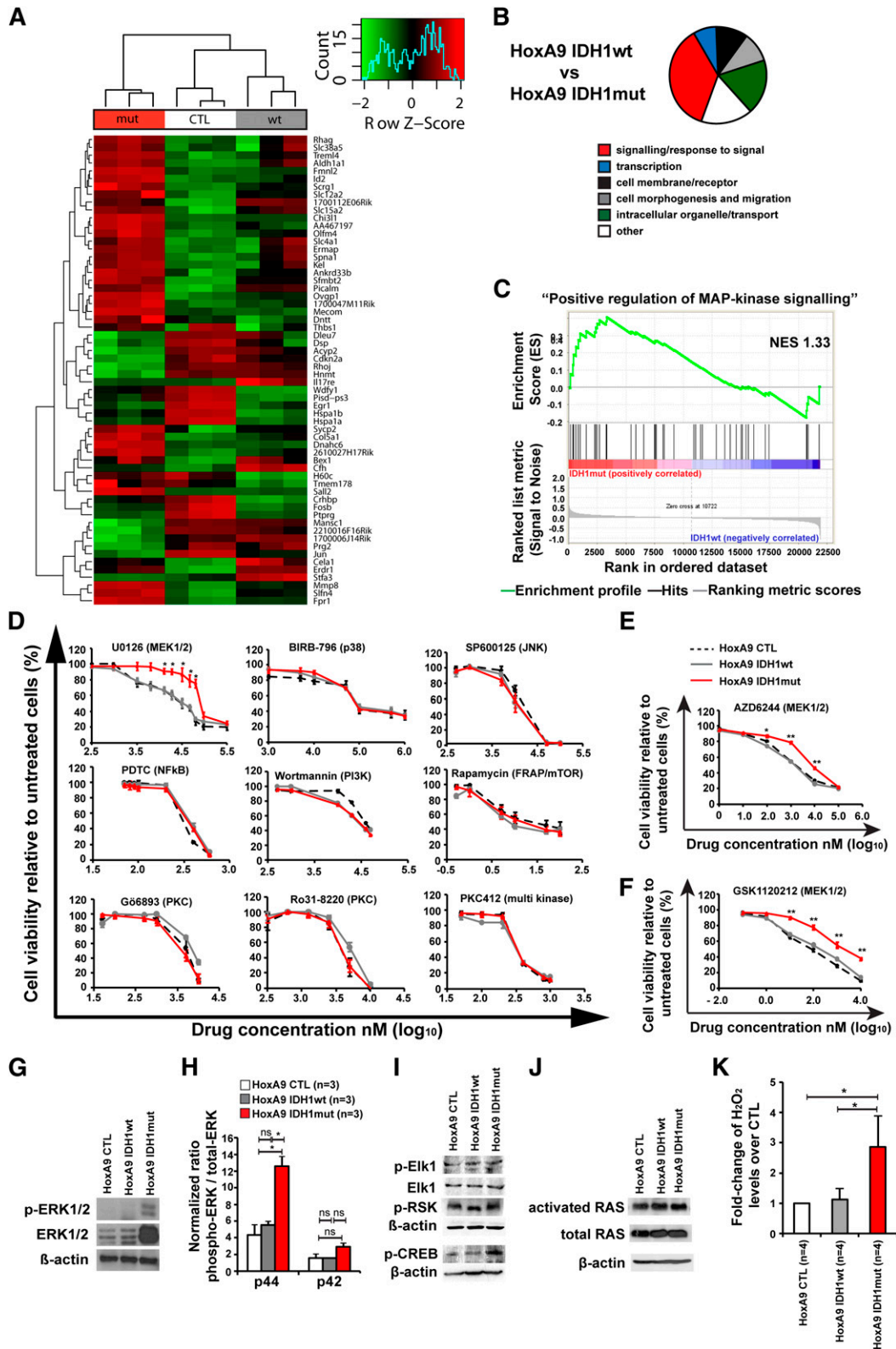
Figure 4. Mutant IDH1 activates MAPK signaling. (A) Row-scaled unsupervised hierarchical clustering of cells transduced with HoxA9 and CTL, IDH1wt, or IDH1mut. Three cell lines per group were generated by independent transductions of bone marrow cells and were transplanted in 1 lethally irradiated mouse each. The cells were harvested from bone marrow 4 weeks after transplantation and were sorted for GFP expression. Gene expression profiling using RNA from sorted cells was performed on Affymetrix Mouse 430.2 arrays. After robust multi-array average normalization, unsupervised hierarchical clustering was performed on variance filtered genes based on a $\log_2$ interquartile range of 1.6. (B) Graphical representation of enriched categories of gene ontology gene sets for the indicated cell comparisons based on gene set enrichment analysis from gene chip arrays. (C) Enrichment plot for the gene set "positive regulation of MAPK signaling" comparing IDH1mut and IDH1wt cells. NES, normalized enrichment score. (D) In vitro cytotoxicity assays using inhibitors of signaling pathways in HoxA9 cells transduced with CTL, IDH1wt, or IDH1mut (mean $\pm$ SEM of 3-5 independent experiments performed in duplicate). (E) In vitro cytotoxicity assay using AZD6244, an inhibitor of MEK1/2 in HoxA9 cells transduced with CTL, IDH1wt, or IDH1mut (mean $\pm$ SEM of 3 independent experiments performed in duplicate). (F) In vitro cytotoxicity assay using GSK1120212, an inhibitor of MEK1/2 in HoxA9 cells transduced with CTL, IDH1wt, or IDH1mut (mean $\pm$ SEM

equal numbers of transgene-positive cells, engraftment in peripheral blood was stable over time (Figure 1D), and complete blood counts (Figure 1E-G), immunophenotype of GFP⁺ cells in peripheral blood (Figure 1H), and spleen weight at 20 weeks after transplantation (Figure 1I) were similar between CTL, IDH1wt, and IDH1mut mice, suggesting that retrovirally expressed mutant IDH1 alone is insufficient to induce myeloproliferation.

To identify other potentially collaborating genes, we compared gene expression levels of known oncogenes between *IDH1*wt and *IDH1*mut AML patients. Eight of 11 *HOXA* cluster genes and 6 of 10 *HOXB* cluster genes were significantly higher expressed in *IDH1* mutant than in wild-type patients (supplemental Figure 1A-B). Overexpression of *HOXA9* in IDH1mut patients was confirmed in an independent patient cohort (supplemental Figure 2). *HOXA9* was independently overexpressed in *IDH1* mutant patients in multivariate analysis including *NPM1*, *FLT3-ITD*, and *CEBPA* mutation status (supplemental Table 1). Because *HOXA9* was most differentially expressed between mutant and wild-type IDH1 patients (Figure 2A), and constitutive *HOXA9* expression induces a long-latency myeloproliferative disease (MPD) in mice,[25,40] we transduced HoxA9-immortalized bone marrow cells with CTL, wild-type, and mutant *IDH1* constructs for in vivo evaluation of their leukemogenic potential (Figure 2B; supplemental Figure 3A-B). A high ratio of *R*-2HG to *S*-2HG in cell lysates from IDH1mut-transduced cells compared with IDH1 wild-type or control cells confirmed the integrity of our model (Figure 2C).

Equal numbers of sorted, GFP⁺ cells were injected in lethally irradiated mice with a life-sparing dose of helper cells. Engraftment of GFP⁺ cells in peripheral blood was higher in IDH1mut-transduced cells at 4, 8, and 12 weeks after transplantation compared with IDH1wt or CTL-transduced cells (Figure 2D). Mice receiving transplants with IDH1-mutated cells developed severe leukocytosis, anemia, and thrombocytopenia after week 4 of transplantation, whereas blood counts in control mice remained normal (Figure 2E-G). Interestingly, IDH1mut mice died with a median latency of 83 days after transplantation, whereas IDH1wt and CTL mice died significantly later (167 and 210 days after transplantation, respectively; IDH1mut vs IDH1wt, $P < .001$; IDH1mut vs CTL, $P < .001$; Figure 2H).

At time of death, the majority of bone marrow cells were derived from IDH1- or CTL-transduced (GFP⁺) cells (supplemental Figure 4A-B). Transduced cells in bone marrow and spleen had a myeloid phenotype predominantly expressing the myeloid marker CD11b and 20% to 30% expressing the progenitor cell marker cKit (supplemental Figure 4C-D). Morphologic evaluation of bone marrow from moribund mice showed that the majority of bone marrow cells had monocytic morphology with an increased proportion of immature cells and slightly more blasts in IDH1mut than in wild-type or CTL mice (Figure 2I-J). Bone marrow cells from moribund mice were readily transplantable into secondary animals with a shorter median survival of IDH1mut compared with IDH1wt mice (supplemental Figure 5). At 2 months after transplantation, no significant difference was observed in GFP⁺lin⁻ckit⁺Sca⁺ and GFP⁺lin⁻ckit⁺Sca⁺CD34⁻ stem and progenitor cells from IDH1wt or IDH1mut mice (supplemental Figure 6A-B). Southern blot

analysis confirmed full proviral integration for each retroviral construct and showed an oligoclonal disease for IDH1mut mice and a monoclonal pattern for IDH1wt mice (supplemental Figure 7). Thus, mutant IDH1 induced a short-latency MPD-like myeloid leukemia in HoxA9-immortalized bone marrow cells, demonstrating its oncogenic potential in vivo.

Mutant IDH1 promotes cell-cycle transition

To assess the biologic effect of mutant IDH1, we compared cell-cycle phases and rate of apoptosis in mutant and wild-type IDH1 cells. Analyzing GFP⁺ bone marrow cells from mice at 9 weeks after transplantation, the rate of apoptosis did not differ between mutated or wild-type IDH1 or CTL transduced cells and was similar to the rate of apoptosis in GFP⁻ cells (supplemental Figure 8A). However, the proportion of cells in S/G2/M phases was significantly higher in bone marrow cells transduced with IDH1mut when compared with cells transduced with IDH1wt or CTL (Figure 3A). The quantitative cell-cycle differences for the HoxA9 immortalized mouse bone marrow cells transduced with CTL, IDH1wt, and IDH1mut cells in vivo are summarized in Figure 3B and in vitro in supplemental Figure 8B.

Gene expression profiles suggested that cyclin-dependent kinase inhibitors were among the most downregulated genes in IDH1mut cells. We quantified gene expression levels of cyclin-dependent kinase inhibitors (*Cdkn*) *1a* (p21), *1b* (p27), *2a* (p16), and *2b* (p15) and found them markedly downregulated in IDH1mut when compared with IDH1wt cells (Figure 3C), providing an explanation for the enhanced cell proliferation in IDH1mut cells. 2HG was previously shown to induce DNA hypermethylation,[17] and silencing of *CDKN2A* and *CDKN2B* expression by promoter hypermethylation has previously been reported in AML.[41] To assess whether *Cdkn2a* and *Cdkn2b* expression was downregulated by promoter methylation in our model, we quantified methylated promoter CpGs by sequencing alleles of bisulfite converted DNA. The CpG island in the promoter of *Cdkn2b* showed low levels of DNA methylation in IDH1wt, IDH1mut, and CTL cells (Figure 3D). The CpG islands in the promoter of *Cdkn2a* showed low levels of DNA methylation in IDH1wt and CTL cells, whereas IDH1mut cells had slightly increased levels of DNA methylation (Figure 3E). These data suggest that mutated IDH1 enhances cell proliferation through reduced expression of CDK inhibitors; however, transcriptional repression rather than gene silencing by promoter methylation seems to be the mechanism for low expression of CDK inhibitors.

Mutant IDH1 activates mitogen-activated protein kinase (MAPK) signaling

To identify pathways that are dysregulated by mutant IDH1, we performed gene expression profiling with cells transduced with HoxA9 and CTL, IDH1wt, or IDH1mut. GFP-expressing cells were harvested from bone marrow 4 weeks after transplantation. In unsupervised hierarchical clustering, mutated cells clustered together and separated from IDH1wt or CTL cells (Figure 4A). Differentially expressed genes are listed in supplemental Table 2. We next performed gene set

Figure 4 (continued) of 3 independent experiments performed in duplicate). (G) Representative western blot of in vitro–cultured cells for the indicated cell lines using antibodies against ERK, phospho-ERK, and β-actin as a loading control. (H) Ratio of phospho-p44 ERK/total-p44 ERK and phospho-p42 ERK/total-p42 ERK in HoxA9 CTL, HoxA9 IDH1wt, and HoxA9 IDH1mut cells (mean ± SEM of 3 independent experiments). (I) Representative western blot of in vitro–cultured cells for the indicated cell lines using antibodies against phospho-Elk1, total Elk1, phospho-p90RSK (Ser380), phospho-CREB, and β-actin as loading control. (J) Representative western blot of in vitro–cultured cells for the indicated cell lines using antibodies against activated RAS, total RAS, and β-actin, as loading control. (K) Hydrogen peroxide levels in cultured cells of the indicated cells that were incubated with Amplex red reaction mixture for 16 hours (mean ± SEM of 4 independent experiments measured in triplicate). *$P < .05$; ns, not significant.

enrichment analysis using the gene sets from gene ontology. Most gene sets were related to membrane receptors, signaling, intracellular organelles and transport, and cell morphogenesis and migration, several of which characterize monocytic function (Figure 4B; supplemental Table 3).

Genes related to MAPK signaling were highly enriched in IDH1 mutant cells (Figure 4C, $P < .001$; supplemental Table 3). To identify whether mutated IDH1 perturbs intracellular signaling as indicated by gene set enrichment analysis, we determined the inhibitory effect of 15 drugs that block a specific signaling pathway. IDH1mut cells were resistant to inhibition with the MEK1/2 inhibitor UO126, which inhibits MAPK signaling, whereas inhibition of JNK, p38, NFkB, PI3-kinase, mTOR, PKC, PLC, PKA-CREB, GSK3β, HIF1-α, Hexokinase, and c-Met was similarly effective in IDH1mut, IDH1wt, and CTL cells (Figure 4D; supplemental Figure 9). Further, IDH1mut cells were also resistant to MEK1/2 inhibitors AZD6244 and GSK 1120212 (Figure 4E-F). Protein levels of ERK and phospho-ERK, and specifically the ratio of phospho-p44/total-p44 were highly upregulated in HoxA9 IDH1mut cells when compared with HoxA9 IDH1wt and HoxA9 CTL cells demonstrating MAPK activation on the protein level (Figure 4G-H; supplemental Figure 10). We also evaluated the effect of mutant IDH1 on ERK in bone marrow cells that do not overexpress HOXA9. Transduced cells were transplanted and sorted from bone marrow after 8 weeks. Total ERK was not increased in mutant IDH1 cells. However, the ratio of phospho-ERK to total ERK was higher by trend ($P = .05$) in mutant IDH1 compared with wild-type IDH1 or control cells for both p44 and p42 isoforms (supplemental Figure 11). We next studied the phosphorylation of downstream and upstream targets of ERK. No difference in phosphorylation levels of Elk-1 and p90RSK (Ser380) was observed between CTL, IDH1wt, and IDH1mut cells (Figure 4I), but phosphorylation of CREB was increased in IDH1mut cells (Figure 4I). Levels of activated RAS and total RAS were similar in CTL, IDH1wt, and IDH1mut cells, suggesting that other signals than RAS activate ERK (Figure 4J). We next assessed whether increased levels of reactive oxygen species (ROS) may be responsible for MEK/ERK activation in IDH1 mutated cells. Indeed, ROS levels were significantly higher in IDH1mut cells compared with IDH1wt or CTL cells (Figure 4K). In summary, mutant IDH1 is associated with enhanced MAPK signaling, possibly through increased ROS levels, and induces resistance against MEK inhibitors.

A novel inhibitor of mutant IDH1 inhibits human AML cell growth

Because inhibition of several signaling pathways did not selectively inhibit IDH1mut cells, we performed a computational drug screen using the ZINC library[39] and the published crystal structure of mutant IDH1. By computational screening we identified a potential inhibitor of mutant IDH1 termed 2-[2-[3-(4-fluorophenyl)pyrrolidin-1-yl]ethyl]-1, 4-dimethylpiperazine (here termed HMS-101). Computational modeling showed that HMS-101 binds to the isocitrate-binding pocket of mutant IDH1 (Figure 5A). The 50% inhibition/inhibitory concentration for HMS-101 was significantly lower in mouse bone marrow cells transduced with IDH1mut compared with IDH1wt (1 μM vs 12 μM, respectively, $P < .001$, Figure 5B). Treatment of HoxA9+IDH1mut cells with HMS-101 at 10 μM significantly reduced intracellular R-2HG levels in vitro (Figure 5C). HMS-101 induced apoptosis in IDH1mut cells as evidenced by Annexin V staining (Figure 5D) and cell-cycle analysis by BrDU (Figure 5E-F). Phospho-ERK1/2 and the ratio of phospho-ERK/total-ERK were markedly reduced in IDH1mut cells compared with IDH1wt or
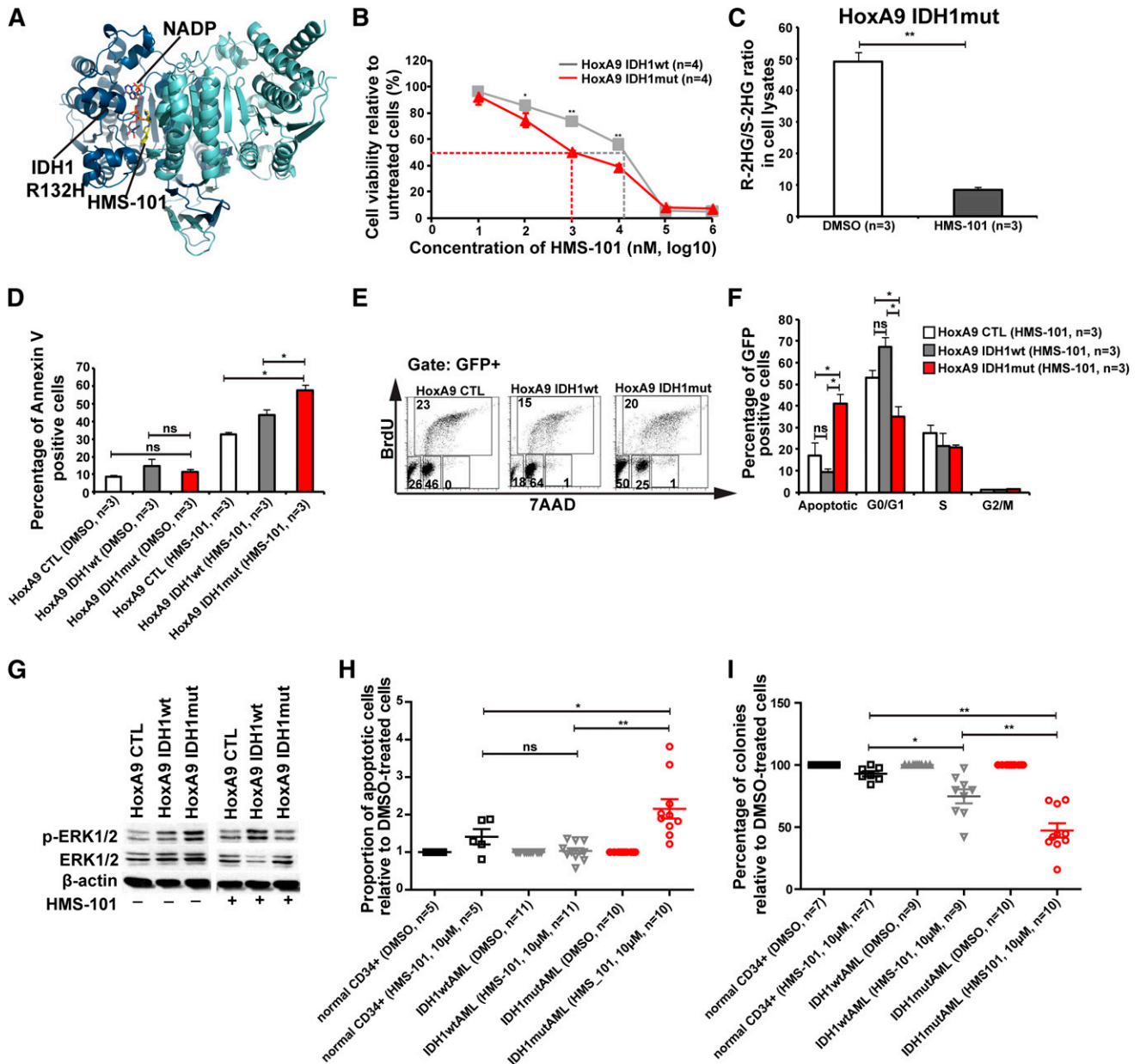
control cells, when treated with HMS-101 (10 μM; Figure 5G; supplemental Figure 12). Next, we evaluated the effect of HMS-101 on human AML cells and CD34^{+} bone marrow cells from healthy donors. Cells were treated in vitro with HMS-101 (10 μM), the highest tolerated dose in normal CD34^{+} human bone marrow cells (supplemental Figure 13) or solvent control for 72 hours to study the rate of apoptosis, or they were plated in methylcellulose in the presence of HMS-101 (10 μM) or solvent control. The percentage of apoptotic cells in HMS-101–treated cells relative to solvent-treated cells was significantly higher in cells from IDH1 mutant patients ($P = .001$), but not in IDH1wild-type ($P = .9$) or CD34^{+} cells from healthy controls ($P = .1$), and was higher in IDH1 mutant patients compared with IDH1 wild-type patients or healthy controls ($P = .001$ and $P = .04$, respectively; Figure 5H). Colony formation in HMS-101–treated cells relative to solvent-treated cells was significantly inhibited in cells from IDH1 mutant patients ($P < .0001$), and also to some extent in IDH1wt patients ($P = .002$), but was not affected in CD34^{+} cells from healthy controls. Colony formation in HMS-101–treated cells was lower in IDH1 mutant patients compared with IDH1 wild-type and control patients ($P = .003$ and $P < .001$, respectively; Figure 5I), suggesting a higher efficacy in IDH1 mutant than in IDH1 wild-type AML. In summary, we identified an inhibitor of mutant IDH1 that shows promising activity in mouse bone marrow cells and in primary human AML cells, suggesting that mutant IDH1 is a relevant and druggable target in AML.

Discussion

We investigated the biologic consequences of constitutive expression of mutant IDH1 in mouse bone marrow cells and found that mutant IDH1 induces a MPD-like myeloid leukemia when combined with HoxA9. Mutant IDH1 accelerated cell-cycle transition possibly by repression of CDK inhibitors, and enhanced MAPK/ERK signaling. A novel inhibitor of mutant IDH1 decreased 2HG production and inhibited progenitor cells from IDH1 mutated AML patients, suggesting that mutant IDH1 is a relevant and druggable target in AML.

In initial experiments, we evaluated the effect of mutant IDH1 alone in vivo. Within 5 months after transplantation, we did not see an engraftment benefit of mutant IDH1 and therefore decided to stop the experiment. Sasaki et al showed that IDH1mut knock-in mice developed splenomegaly and increased levels of hematopoietic stem cells in older mice, but did not die of myeloid disease within 2 years of observation.[23] Because of the relatively short observation period in our study, we may have missed such an effect of mutant IDH1. However, we focused on collaborating oncogenes to mimic the physiologic situation in AML patients, where several mutations may co-occur. Based on an initial report that mutant *IDH1* was associated with *HOX* gene overexpression,[18] we confirmed this association in 2 large cohorts of AML patients and selected HOXA9 as a potential cooperating oncogene.

We found that mutant IDH1 in combination with HoxA9 accelerates the onset of an MPD. Following Bethesda criteria, we termed the disease MPD-like myeloid leukemia.[42] The contribution of mutant IDH1 to the disease phenotype seems to be enhanced cell proliferation as evidenced by a rapid increase in white blood cell counts and spleen weight in transplanted mice, an increased proportion of cells in S/G2/M phases of cell cycle in vivo and in vitro, and shorter disease latency in primary and secondary transplants. The frequency of hematopoietic stem cells was similar between mutant and wild-type IDH1 and controls, likely because of

Figure 5. A novel inhibitor of mutant IDH1 inhibits human AML cell growth. (A) Structural model of the IDH1R132H dimer showing binding of HMS-101 and NAD phosphate (NADP) to the active center of IDH1. (B) Cell viability of HoxA9+IDH1wt and HoxA9+IDHmut cells incubated with increasing concentrations of HMS-101 (mean ± SEM of 4 independent experiments). (C) Ratio of R-2HG and S-2HG in HoxA9+IDHmut-transduced bone marrow cells incubated with 10 μM HMS-101 for 72 hours (mean ± SEM, n = 3). (D) Induction of apoptosis by HMS-101 (10 μM) indicated by the proportion of annexin V positive cells in murine bone marrow cells transduced with HoxA9 CTL, HoxA9 IDH1wt, and HoxA9 IDH1mut after 72 hours of treatment (mean ± SEM, n = 3). (E) Representative FACS blots of cell-cycle phases in HoxA9 CTL, HoxA9 IDH1wt, and HoxA9 IDH1mut cells treated with HMS-101 (10 μM) for 72 hours. Cell-cycle phases were determined by analysis of BrdU/7AAD-stained cells by FACS. The upper quadrant represents cells in S phase, the lower left quadrant represents apoptotic cells, the lower middle quadrant represent cells in G0/G1 phase, and the lower right quadrant represents cells in G2/M phase of the cell cycle. (F) Quantitative analysis of cell-cycle distribution after treatment with HMS-101 (10 μM) in the HoxA9 CTL, HoxA9 IDH1wt, and HoxA9 IDH1mut cell lines for 72 hours as described in Figure 5E (mean ± SEM, n = 3). (G) Representative western blot of in vitro–cultured cells treated with HMS-101 for the indicated murine cell lines using antibodies against phospho-ERK, total-ERK, and β-actin as loading control. (H) Induction of apoptosis by HMS-101 (10 μM) in the indicated cell types relative to dimethylsulfoxide (DMSO)-treated cells after suspension culture for 72 hours. (I) Inhibition of colony formation in CFC assays using human cells from healthy donors or AML patients with wild-type or mutant IDH1 by HMS-101 relative to DMSO-treated cells (mean ± SEM). *P < .05; **P < .01; ns, not significant.

the fairly differentiated monocytic phenotype of HoxA9-expressing cells that dominated the morphology of all groups.

We observed a slight increase in bone marrow blasts in mutant IDH1 cells, suggesting that mutant IDH1 has an inhibitory effect on differentiation. Previous studies showed that mutant IDH1 blocks myeloid and adipocyte differentiation,[17,20] as evidenced by an increased cKit expression in CFCs from mouse bone marrow transduced

with mutant IDH2, when compared with wild-type IDH2,[17] and reduced lipid droplet accumulation in 3T3-L1 cells transduced with IDH2R172K when compared with either wild-type IDH2 or vector control.[20]

By gene set enrichment analysis in our study, we found MAPK signaling most upregulated in mutant IDH1 cells. Western blot analysis of ERK1/2 and pharmacologic inhibition of MAPK signaling

supported activation of the MAPK pathway, whereas inhibition of many other signaling pathways did not show differential sensitivity in mutant or wild-type cells. MAPK signaling was also upregulated in a previous study in melanoma cells ectopically expressing mutated IDH1.[8] We found that IDH1mut cells generated increased levels of ROS, which are known to activate MAPK signaling. Previous studies have shown that elevated 2HG levels resulted in increased ROS levels[43,44]; altered reduced NAD phosphate metabolism resulting from mutated IDH1 could further exacerbate this effect. Two previous studies measured ROS levels in IDH1 mutated cells and did not find elevated levels of ROS.[8,23] This discrepancy may be due to different methods that were used in these studies. ROS levels were measured by CM-H$_2$DCFDA staining in the negative studies, which has 35- and 39-fold lower reactivity to H$_2$O$_2$ than to the hydroxyl radical and peroxynitrite anion, respectively,[45] whereas Amplex red was used in our study reacting primarily with H$_2$O$_2$. Alternatively, ROS levels and MAPK signaling may be increased due to enhanced cell proliferation.[46]

A recent study showed that mutant IDH1 induces cytokine independence in the leukemia cell line TF1. Interestingly, this effect was also seen when cells were treated with R-2HG, but not when treated with S-2HG,[22] demonstrating the biologic relevance of R-2HG. To explore whether inhibition of the enzymatic function of mutated IDH1 had antileukemic effects, we searched for specific IDH1 inhibitors using an in silico screening platform. One of our hits with high affinity to mutated IDH1 demonstrated promising activity in vitro on cell proliferation and ERK signaling. The specificity of the IDH1 inhibitor HMS-101 was shown by reduction of R-2HG levels in IDH1 mutant cells. The inhibitor enhanced apoptosis and inhibited colony formation in murine cells and primary AML cells from IDH1 mutated patients. Colony formation was also reduced in some AML patients with wild-type IDH1, but not in CD34$^+$ bone marrow cells from healthy donors. This data suggest that primary AML cells depend on mutated IDH1, that targeting of IDH1 may have therapeutic benefit, and that mutant IDH1 can be effectively targeted in human AML cells.

In summary, mutant IDH1 cooperates with HOXA9 to induce a MPD-like myeloid leukemia and enhances cell proliferation possibly through repression of CDK inhibitors. Pharmacologic inhibition of 2HG production inhibits AML cell survival and suggests that mutant IDH1 is a relevant therapeutic target in AML.

Authorship

Contribution: A.C. and M.H. designed the research; A.C., M.M.A.C., N.J., A.S., H.Y., K.G., M.W., A.S., M.P., F.T., J.M., R.H., E.A.S., E.E.J., U.M., Z.L., L.M.S., R.G., R.L., and U.L. performed the research; F.T., J.K., A.G., and M.H. contributed patient samples and clinical data; A.C., M.M.A.C., N.J., A.S., M.P., F.T., J.M., E.A.S., R.G., D.J.M., U.L., J.K., A.G., and M.H. analyzed the data; A.C. and M.H. wrote the manuscript; and all authors read and agreed to the final version of the manuscript.

Conflict-of-interest disclosure: A.C., M.P., and M.H. have filed a patent for clinical and research use of drug HMS-101. The remaining authors declare no competing financial interests.

Correspondence: Michael Heuser, Department of Hematology, Hemostasis, Oncology, and Stem Cell Transplantation, Hannover Medical School, Carl-Neuberg Strasse 1, 30625 Hannover, Germany; e-mail: heuser.michael@mh-hannover.de.

References

1. Parsons DW, Jones S, Zhang X, et al. An integrated genomic analysis of human glioblastoma multiforme. *Science.* 2008; 321(5897):1807-1812.

2. Yan H, Parsons DW, Jin G, et al. IDH1 and IDH2 mutations in gliomas. *N Engl J Med.* 2009;360(8): 765-773.

3. Mardis ER, Ding L, Dooling DJ, et al. Recurring mutations found by sequencing an acute myeloid leukemia genome. *N Engl J Med.* 2009;361(11): 1058-1066.

4. Green A, Beer P. Somatic mutations of IDH1 and IDH2 in the leukemic transformation of myeloproliferative neoplasms. *N Engl J Med.* 2010;362(4):369-370.

5. Thol F, Weissinger EM, Krauter J, et al. IDH1 mutations in patients with myelodysplastic syndromes are associated with an unfavorable prognosis. *Haematologica.* 2010;95(10): 1668-1674.

6. Amary MF, Bacsi K, Maggiani F, et al. IDH1 and IDH2 mutations are frequent events in central chondrosarcoma and central and periosteal chondromas but not in other mesenchymal tumours. *J Pathol.* 2011;224(3):334-343.

7. Cairns RA, Iqbal J, Lemonnier F, et al. IDH2 mutations are frequent in angioimmunoblastic T-cell lymphoma. *Blood.* 2012;119(8):1901-1903.

8. Shibata T, Kokubu A, Miyamoto M, Sasajima Y, Yamazaki N. Mutant IDH1 confers an in vivo growth in a melanoma cell line with BRAF mutation. *Am J Pathol.* 2011;178(3):1395-1402.

9. Murugan AK, Bojdani E, Xing M. Identification and functional characterization of isocitrate dehydrogenase 1 (IDH1) mutations in thyroid cancer. *Biochem Biophys Res Commun.* 2010; 393(3):555-559.

10. Wagner K, Damm F, Göhring G, et al. Impact of IDH1 R132 mutations and an IDH1 single nucleotide polymorphism in cytogenetically normal acute myeloid leukemia: SNP rs11554137

is an adverse prognostic factor. *J Clin Oncol.* 2010;28(14):2356-2364.

11. Thol F, Damm F, Wagner K, et al. Prognostic impact of IDH2 mutations in cytogenetically normal acute myeloid leukemia. *Blood.* 2010; 116(4):614-616.

12. Paschka P, Schlenk RF, Gaidzik VI, et al. IDH1 and IDH2 mutations are frequent genetic alterations in acute myeloid leukemia and confer adverse prognosis in cytogenetically normal acute myeloid leukemia with NPM1 mutation without FLT3 internal tandem duplication. *J Clin Oncol.* 2010;28(22):3636-3643.

13. Marcucci G, Maharry K, Wu YZ, et al. IDH1 and IDH2 gene mutations identify novel molecular subsets within de novo cytogenetically normal acute myeloid leukemia: a Cancer and Leukemia Group B study. *J Clin Oncol.* 2010;28(14): 2348-2355.

14. Gross S, Cairns RA, Minden MD, et al. Cancer-associated metabolite 2-hydroxyglutarate accumulates in acute myelogenous leukemia with

isocitrate dehydrogenase 1 and 2 mutations. *J Exp Med.* 2010;207(2):339-344.

15. Dang L, White DW, Gross S, et al. Cancer-associated IDH1 mutations produce 2-hydroxyglutarate. *Nature.* 2009;462(7274): 739-744.

16. Ward PS, Patel J, Wise DR, et al. The common feature of leukemia-associated IDH1 and IDH2 mutations is a neomorphic enzyme activity converting alpha-ketoglutarate to 2-hydroxyglutarate. *Cancer Cell.* 2010;17(3): 225-234.

17. Figueroa ME, Abdel-Wahab O, Lu C, et al. Leukemic IDH1 and IDH2 mutations result in a hypermethylation phenotype, disrupt TET2 function, and impair hematopoietic differentiation. *Cancer Cell.* 2010;18(6):553-567.

18. Xu W, Yang H, Liu Y, et al. Oncometabolite 2-hydroxyglutarate is a competitive inhibitor of α-ketoglutarate-dependent dioxygenases. *Cancer Cell.* 2011;19(1):17-30.

19. Koivunen P, Lee S, Duncan CG, et al. Transformation by the (R)-enantiomer of 2-hydroxyglutarate linked to EGLN activation. *Nature.* 2012;483(7390):484-488.

20. Lu C, Ward PS, Kapoor GS, et al. IDH mutation impairs histone demethylation and results in a block to cell differentiation. *Nature.* 2012; 483(7390):474-478.

21. Chowdhury R, Yeoh KK, Tian YM, et al. The oncometabolite 2-hydroxyglutarate inhibits histone lysine demethylases. *EMBO Rep.* 2011; 12(5):463-469.

22. Losman JA, Looper RE, Koivunen P, et al. (R)-2-hydroxyglutarate is sufficient to promote leukemogenesis and its effects are reversible. *Science.* 2013;339(6127):1621-1625.

23. Sasaki M, Knobbe CB, Munger JC, et al. IDH1(R132H) mutation increases murine haematopoietic progenitors and alters epigenetics. *Nature.* 2012;488(7413):656-659.

24. Chou WC, Hou HA, Chen CY, et al. Distinct clinical and biologic characteristics in adult acute myeloid leukemia bearing the isocitrate dehydrogenase 1 mutation. *Blood.* 2010;115(14): 2749-2754.

25. Kroon E, Krosl J, Thorsteinsdottir U, Baban S, Buchberg AM, Sauvageau G. Hoxa9 transforms primary bone marrow cells through specific collaboration with Meis1a but not Pbx1b. *EMBO J.* 1998;17(13):3714-3725.

26. Schambach A, Wodrich H, Hildinger M, Bohne J, Kräusslich HG, Baum C. Context dependence of different modules for posttranscriptional enhancement of gene expression from retroviral vectors. *Mol Ther.* 2000;2(5):435-445.

27. Heuser M, Yun H, Berg T, et al. Cell of origin in AML: susceptibility to MN1-induced transformation is regulated by the MEIS1/AbdB-like HOX protein complex. *Cancer Cell.* 2011; 20(1):39-52.

28. Gurevich RM, Aplan PD, Humphries RK. NUP98-topoisomerase I acute myeloid leukemia-associated fusion gene has potent leukemogenic activities independent of an engineered catalytic site mutation. *Blood.* 2004;104(4):1127-1136.

29. Heuser M, Sly LM, Argiropoulos B, et al. Modeling the functional heterogeneity of leukemia stem cells: role of STAT5 in leukemia stem cell self-renewal. *Blood.* 2009;114(19):3983-3993.

30. Heuser M, Argiropoulos B, Kuchenbauer F, et al. MN1 overexpression induces acute myeloid leukemia in mice and predicts ATRA resistance in patients with AML. *Blood.* 2007;110(5): 1639-1647.

31. Abbas S, Lugthart S, Kavelaars FG, et al. Acquired mutations in the genes encoding IDH1 and IDH2 both are recurrent aberrations in acute myeloid leukemia: prevalence and prognostic value. *Blood.* 2010;116(12):2122-2126.

32. Ley TJ, Miller C, Ding L, et al. Genomic and epigenomic landscapes of adult de novo acute myeloid leukemia. *N Engl J Med.* 2013;368(22): 2059-2075.

33. Struys EA, Jansen EE, Verhoeven NM, Jakobs C. Measurement of urinary D- and L-2-hydroxyglutarate enantiomers by stable-isotope-dilution liquid chromatography-tandem mass spectrometry after derivatization with diacetyl-L-tartaric anhydride. *Clin Chem.* 2004;50(8): 1391-1395.

34. Scherr M, Chaturvedi A, Battmer K, et al. Enhanced sensitivity to inhibition of SHP2, STAT5, and Gab2 expression in chronic myeloid leukemia (CML). *Blood.* 2006;107(8):3279-3287.

35. Heuser M, Beutel G, Krauter J, et al. High meningioma 1 (MN1) expression as a predictor for poor outcome in acute myeloid leukemia with normal cytogenetics. *Blood.* 2006;108(12): 3898-3905.

36. Heuser M, Yap DB, Leung M, et al. Loss of MLL5 results in pleiotropic hematopoietic defects, reduced neutrophil immune function, and extreme sensitivity to DNA demethylation. *Blood.* 2009; 113(7):1432-1443.

37. Livak KJ, Schmittgen TD. Analysis of relative gene expression data using real-time quantitative PCR and the 2(-Delta Delta C(T)) Method. *Methods.* 2001;25(4):402-408.

38. Sali A, Blundell TL. Comparative protein modelling by satisfaction of spatial restraints. *J Mol Biol.* 1993;234(3):779-815.

39. Irwin JJ, Sterling T, Mysinger MM, Bolstad ES, Coleman RG. ZINC: a free tool to discover chemistry for biology [published online ahead of print June 15, 2012]. *J Chem Inf Model.*

40. Heuser M, Berg T, Kuchenbauer F, et al. Functional role of BAALC in leukemogenesis. *Leukemia.* 2012;26(3):532-536.

41. Wong IH, Ng MH, Huang DP, Lee JC. Aberrant p15 promoter methylation in adult and childhood acute leukemias of nearly all morphologic subtypes: potential prognostic implications. *Blood.* 2000;95(6):1942-1949.

42. Kogan SC, Ward JM, Anver MR, et al; Hematopathology subcommittee of the Mouse Models of Human Cancers Consortium. Bethesda proposals for classification of nonlymphoid hematopoietic neoplasms in mice. *Blood.* 2002; 100(1):238-245.

43. Kölker S, Pawlak V, Ahlemeyer B, et al. NMDA receptor activation and respiratory chain complex V inhibition contribute to neurodegeneration in d-2-hydroxyglutaric aciduria. *Eur J Neurosci.* 2002;16(1):21-28.

44. Latini A, Scussiato K, Rosa RB, et al. D-2-hydroxyglutaric acid induces oxidative stress in cerebral cortex of young rats. *Eur J Neurosci.* 2003;17(10):2017-2022.

45. Setsukinai K, Urano Y, Kakinuma K, Majima HJ, Nagano T. Development of novel fluorescence probes that can reliably detect reactive oxygen species and distinguish specific species. *J Biol Chem.* 2003;278(5):3170-3175.

46. Sallmyr A, Fan J, Datta K, et al. Internal tandem duplication of FLT3 (FLT3/ITD) induces increased ROS production, DNA damage, and misrepair: implications for poor prognosis in AML. *Blood.* 2008;111(6):3173-3182.